

Pre-slippage detection and counter-slippage for e-pattern omniwheeled cellular conveyor

Joe Siang Keek¹, Ser Lee Loh¹, Ainain Nur Hanafi¹, Tau Han Cheong²

¹Fakulti Teknologi dan Kejuruteraan Elektrik, Universiti Teknikal Malaysia Melaka, Melaka, Malaysia

²Fakulti Pendidikan, Universiti Teknologi MARA, Cawangan Selangor, Malaysia

Article Info

Article history:

Received Jun 15, 2023

Revised Sep 2, 2023

Accepted Nov 14, 2023

Keywords:

Cellular
Conveyor
Modular
Omnidirectional
Omn wheel
Slippage

ABSTRACT

This paper presents continuation work of e-pattern omniwheeled cellular conveyor (EOCC) since its first introduction. EOCC is a conveyor that is modular and is made up of omniwheels arranged horizontally and vertically. Although in the last published paper, the EOCC had been proven to be capable of transporting box omnidirectionally and achieving yaw control concurrently, however, due to the natural properties of omniwheel, the performance is jeopardized by slippage. While minor slippage can be negligible, but a major slippage can eventually destroy the whole trajectory tracking performance. Therefore, counter-slippage methods are proposed in this paper. The simulation results show that the proposed counter-slippage method significantly improves the trajectory tracking performance up to 42% of reduction in integral of absolute error. Moreover, in this paper, pre-slippage detection method, which aims to perform early detection of slippage, is being presented as well. Although these proposed methods are simple, but they are proven to have achieved improved tracking performance than conventional controller, as presented in this paper.

This is an open access article under the [CC BY-SA](#) license.



Corresponding Author:

Ser Lee Loh

Fakulti Teknologi dan Kejuruteraan Elektrik, Universiti Teknikal Malaysia Melaka

Jalan Hang Tuah Jaya, Durian Tunggal, Melaka, 76100, Malaysia

Email: slloh@utem.edu.my

1. INTRODUCTION

Conventional conveyor system is usually made up of roller or belt for unidirectional transportation of item. Additionally, hydraulic-or pneumatic-powered linear actuator was introduced to enable change of direction during transportation. Such conventional setup has very limited capability in term of position and orientation controls. Moreover, when there is a breakdown in one of the actuators or rollers, whole logistic line needs to be paused for maintenance. This could potentially jeopardize the throughput of the production line. Therefore, omnidirectional cellular conveyor (OCC) has been actively discussed in the field of research [1]. It can be considered one of the cutting-edge technology and automation in the field of logistics.

Omnidirectional and modular (or cellular) are the fundamental and compulsory features of OCC. Unlike conventional conveyor technology that requires additional actuators, OCC is capable of transporting box omnidirectionally i.e., positioning or velocity control and yaw (orientation) control concurrently, and having multiple inbounds and multiple outbounds. Moreover, multiple boxes can be transported at the same time as well at any desired direction and orientation. Such feature is highly favourable for industries that involves sorting. In fact, most of the industries nowadays involve sorting of their products [2]–[4]. Next, OCC is a conveyor system that is modular. Usually in conventional belt conveyor, when the main driving rotor fails, or one of the linear actuators stop functioning properly, the whole transportation line must be paused. However, in the working principle of OCC, when one of its cells or modules is not working, it can

then be bypassed, and the incoming box can be temporarily handled by neighbouring modules. Moreover, since OCC is modular, the faulty module can be replaced quickly in just a plug-and-play manner [5]. These two main specialties of OCC are sufficient to deduce that OCC is a research-worthy topic and a futuristic technology [6]. Figure 1 shows the basic working principle of OCC (Figure 1(a)) and conventional conveyor (Figure 1(b)).

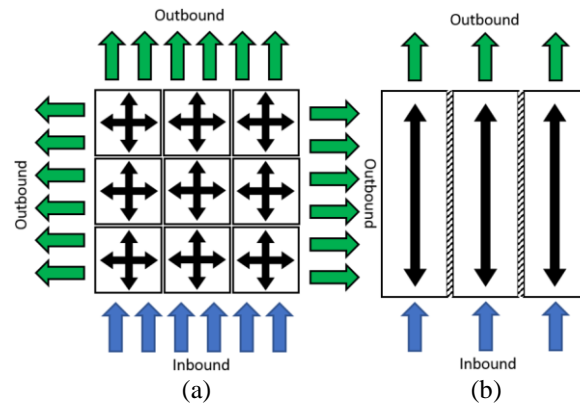


Figure 1. Working principle of: (a) OCC and (b) conventional conveyor

Even though the invention of omnidirectional wheel such as omniwheel [7] and Mecanum wheel [8] happened over half century ago, but the proposal and development of OCC-related research has only been started since around two decades ago. They can be classified to either omnidirectional conveyor (OC), cellular conveyor (CC) or OCC. Oyobe *et al.* [9] proposed an OC known as ‘Magic Carpet’, which is made up of multiple z-directional actuators. Controlling these actuators create a steep surface for box to gain potential energy for transportation. Another OC that is made up of omniwheels known as rotacaster material handling (RMH) was proposed [3]. RMH utilizes omniwheels to transport different semiconductor wafers easy sorting without any jamming on the conveyor. Next, small-scaled conveyor module (SCM) [10]–[13] and Celluveyor [12] are two OCC that are available in the literature. SCM module is made up of single wheel that has extra degree of freedom that can swivel the wheel to certain angle to change the direction of the travel. In one of the recent research studies, a similar swivelling idea but using gravity instead of driving wheel is proposed, which is known as under-actuated smart surface.

One can expect that the control system designed for OCC is a difficult task as it involves multiple actuators that need to cooperatively work with each other, together with multiple sensors (decentralized control system) or single sensor (centralized control system). Additionally, filtering are compulsory most of the time for fusion of sensory data [14], [15]. Therefore, achieving precise positioning and orientation controls for OCC are undeniably challenging. A decentralized control system (DCS) usually has sensors built within every module. Communication happens from module to module to convey the box. In DCS, each module has microprocessor on board to control its own actuation [10], [11], [16], [17]. Whereas for centralized control system (CCS), a centralized processing unit will be controlling the actuation of all the modules on its own. CCS usually have the overview of the whole conveyor system either through bird’s-eye view camera or feedback from all on-module sensor [12], [18]. Both DCS and CCS has respective pros and cons. SCM and Celluveyor are the examples of DCS and CCS, respectively.

Since OCC is a complex system that involves sensor data and continuous control of all the actuators in a cooperative manner, therefore, designing a control system for it is a challenging task. Literature study shows that there is limited detailed discussion about the control system or controller designed for their proposed OCC. ‘Magic Carpet’ has proportional-derivative (PD) controller with disturbance observer used to control the flow of the conveying box [9]. For Celluveyor, PD controller is used as well, but for velocity and angle controls. Kinematic modelling of Celluveyor-like of OCC can be found in [18], [19].

E-pattern omniwheeled cellular conveyor (EOCC) is an OCC working under CCS. EOCC was first introduced and discussed in [20]. The proposal of EOCC is not a wheel-reinvention but instead, EOCC aims to have higher resolution and higher precision control over positioning control and orientation control, regardless the size and mass of the conveying boxes. After all, the contribution of EOCC and its control system in this paper aim to elevate the benchmark and competitiveness among other modern conveyor technologies, with ultimate goal of enabling the technology towards maturity and wide implementation in the industry.

2. E-PATTERN OMNIWHEELED CELLULAR CONVEYOR

EOCC consists of modules with omniwheels that has either diameter of 17.2 cm or 6.2 cm. The bigger omniwheels are always perpendicular with the smaller omniwheels, thus overall creating an arrangement that look like alphabet 'E'. Figure 2 shows the physical appearance of EOCC module and how the modules are arranged for this research experiments. Figure 2(a) shows single module of EOCC and Figure 2(b) shows multiple modules arranged in 6×7 array. Similar with Grabowiecki [20], the modelling of the omniwheels and experiments are done by using a robotic software known as virtual robot experimentation platform (V-REP), now known as coppeliasim.

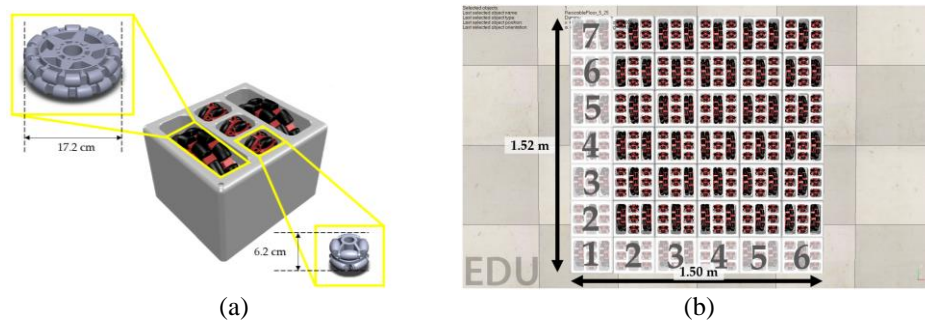


Figure 2. EOCC: (a) in single module and (b) arranged in a 6×7 array form

In simulation environment, a bird's eye view camera is placed on top of the EOCC. Unlike most of the conventional OCC which has auxiliary dead-reckoning or object detection sensor, EOCC solely relies on the image feedback from the camera. Nowadays, image processing has become a norm to most of the robotic application [12], [18], [21], [22]. In EOCC, raw image was first obtained, scaled down and then grayscaled for the purpose of lightweight processing. Each detected omniwheels in the image are drawn with a bounding box, each of the wheels are assigned with a unique address. The program developed uses these addresses to control the actuation of each wheel. The absolute position and orientation of box is determined by using image processing technique as well. Figure 3 shows a series of images on how the images processing is done. Figures 3(a) to (c) shows the omniwheels are detected and processed, and localization of the box by machine vision of EOCC. Whereas Figure 3(d) demonstrates activation of omniwheels during motion control.

Since most of the OCC involves large number of actuators, therefore, it is vital to have an energy-efficient control plan. In EOCC, a method known as 'cross-then-activate' is used. The idea is to only activate the omniwheels when the box is nearby to it i.e., crossing the bounding box. So, by that time when the box reaches the point of contact of the wheel, which is the centre of the bounding box, the box can be efficiently transported in a smooth motion. Figure 3(d) shows a sample implementation 'cross-then-activate' method, whereby green colour bounding box represents active omniwheel at that particular instant.

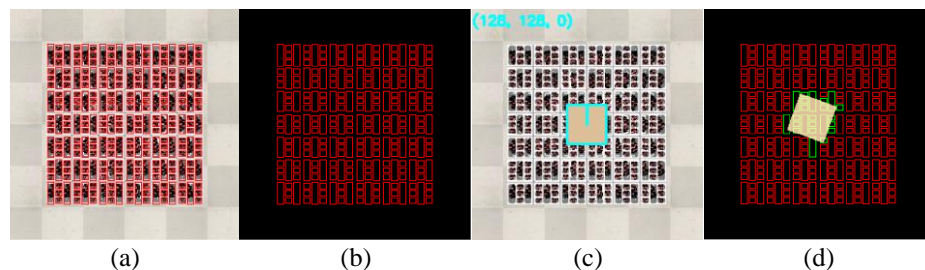


Figure 3. Images of: (a) detected omniwheels with bounding box, (b) post-processed for lightweight processing, (c) localization of the detected box, and (d) actual control and vision by computer

2.1. Control system

Once the sensor and actuator are all ready, a Python language program is developed to create a closed loop for the EOCC. Figure 4 shows the block diagram of the EOCC. First, at the feedback path, it has

the positioning and orientation data feedback from the image processor. The feedback data, $A'(k)$ is then compared with input, $R(k)$ to create a delta value, $e(k)$. This delta value is then used by controller to control the magnitude of the actuators. Two proportional (P) controllers are used to control x-axis (small omniwheels) and y-axis (big omniwheels) motions. Whereas for orientation control, another two P controllers are used to control big omniwheels and small omniwheels respectively during orientation control. In the block diagram in Figure 4, the 'Rotation direction decoder' is an algorithm that decides the direction of rotation of the wheels by using the location of the wheels with respect to the centre of the box. The illustrated example that shows the direction of the wheels' rotation when the box is needed to rotate clockwise can be seen in Figure 4 highlighted with green. At the end of the block diagram, all the controllers' outputs are summed to create a resultant force that convey box towards desired position and desired orientation.

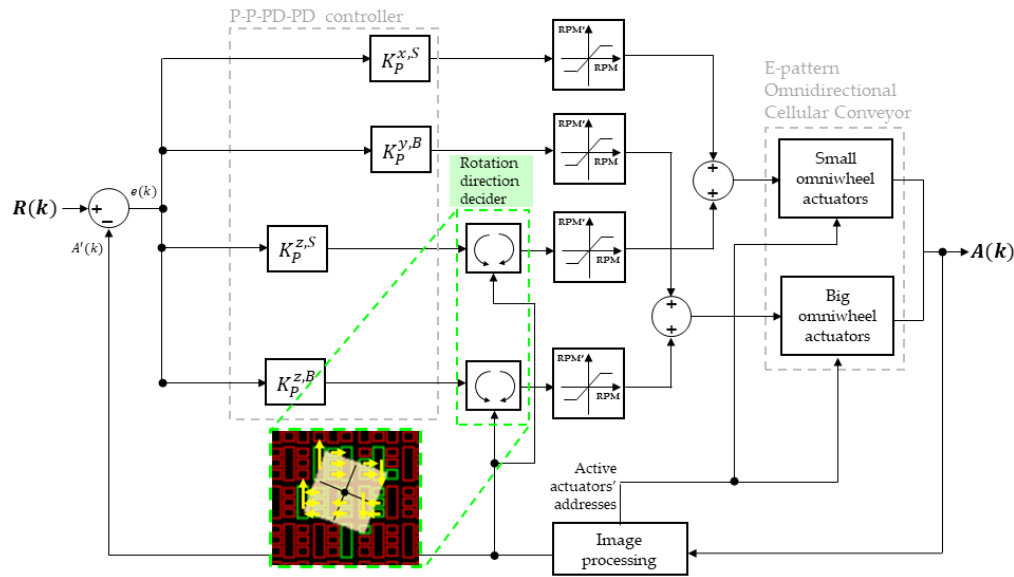


Figure 4. Block diagram of EOCC control system

Ziegler-nichols (ZN) method is a well-known method used to tune proportional-integral-derivative (PID) controller [23]. This is due to its simplicity in getting the controller ready in basic form. However, the outcome by the tuning method is usually not robust towards system nonlinearity and system variation most of the time. Since in this paper, the mass and size are constant throughout the experiments, therefore, ZN method can be used to tune the controller shown in the block diagram. Proportional gain of X-direction (Figure 5(a)) and Y-direction (Figure 5(b)) controllers were slowly increased until an oscillatory response is obtained as shown in Figure 5.

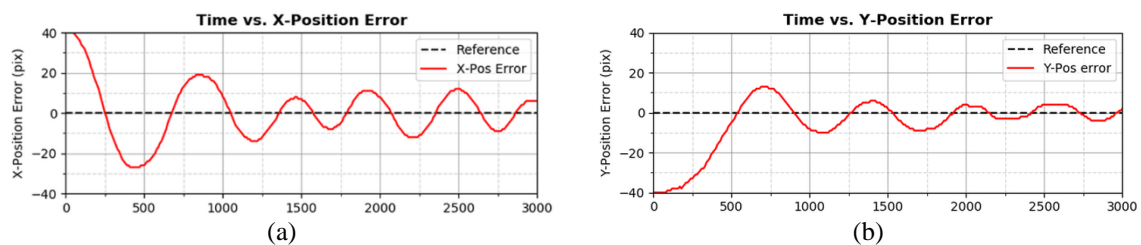


Figure 5. Non-damping oscillatory response in: (a) horizontal and (b) vertical motion during ZN tuning

When such nondecaying oscillatory response is obtained, critical gain value, K_U is then determined. ZN-tuned proportional gain K_p can then be calculated by using ZN formula as shown as (1):

$$K_p = \frac{K_U}{0.5} \quad (1)$$

To successfully achieve desired positioning and orientation controls, a group of omniwheels must cooperatively work together in creating a harmonized and controlled resultant motion towards desired trajectory. Moreover, the number of wheels involved and their point of contact with the box are changing throughout the whole transporting process. To determine the system uncertainty and system nonlinearity of the EOCC, it is therefore important to first study the nominal characteristic of the EOCC. Similar with [24], open-loop step response is used to understand the nominal characteristic of the EOCC. The outcome of the step responses is as shown in Figure 6. Based on Figure 6(a), it can be noticed that the system (the small omniwheels of the EOCC in this case) shows insignificant nonlinearity under different actuator gain values, ranges from 2.0 up to 16.0 with step value of 2.0. However, based on Figure 6(b), it can be noticed that the big omniwheels of the EOCC has significant nonlinear characteristic—the relationship between motor gain values and distance travelled is not proportional, and significant system uncertainty—fluctuating velocity during the conveying period. Anyhow, this is understandable because unlike X-direction control which involves at least six omniwheels (the small omniwheels), the transportation in Y-direction involves only two omniwheels (the big omniwheels). The lesser the number of contact point, the lesser the friction and therefore, the higher the chance for slippage to happen. This is exactly the situation of the EOCC Y-direction transportation. Afterall, it is not surprising that omniwheels are highly prone towards slippage [25]–[27]. Solution to overcome the slippage has always been a hot topic to discuss in the literature. In the upcoming sub-section, counter-slippage method is proposed and discussed for the EOCC.

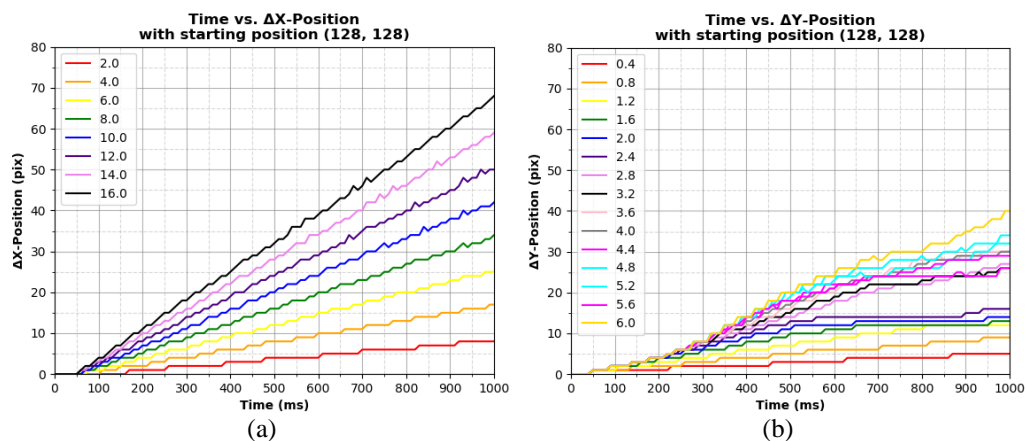


Figure 6. Open-loop step response in: (a) X-direction (horizontal) under different motor gain values and (b) Y-direction (vertical) under different motor gain values

2.2. Counter slippage

Slippage among omniwheel has always been a widely discussed topic since the first invention of the wheel. Studies had been conducted on understanding the characteristic of the wheel such as determining the shift of contact point, and compression of the rubber roller on the wheels [26], [27], just to name a few. To counteract this drawback, efforts such as mathematical modelling of slippage [28], [29], adaptive control system [30], and time-varying controller [31], were proposed in the literature. As mentioned in the last section, EOCC is also experiencing slippage. Therefore, in this paper, a counter-slippage method is proposed. This method forcibly inputs the following rotation motion as illustrated in Figure 7, to ‘shake’ the box out from slippage trap. Figures 7(a) and (b) show counter-slippage input signal in symmetrical triangular form and asymmetrical triangular form, respectively. This proposed method uses a triangular input signal is because by comparing with sinusoidal signal which has slower rising curve, triangular signal is more effective in quickly removing the box out from slippage trap.

It is important to re-iterate that this triangular signal is applied on yaw motion control only. Thus, it will cause the box to yaw in clockwise direction and then followed by anticlockwise direction during conveying transportation. Such triangular motion performs a ‘shakeout’ to the box, either preventing or saving the box out from immovable slippage trap. The total period of the counter-slippage signal lasts less than 1 second as shown in Figure 7. This because the counter-slippage is intended to be quick and effective, yet without jeopardizing too much on positional precision during the transportation (trajectory tracking). The result and effectiveness of the proposed counter-slippage method are discussed in section 4 of this paper.

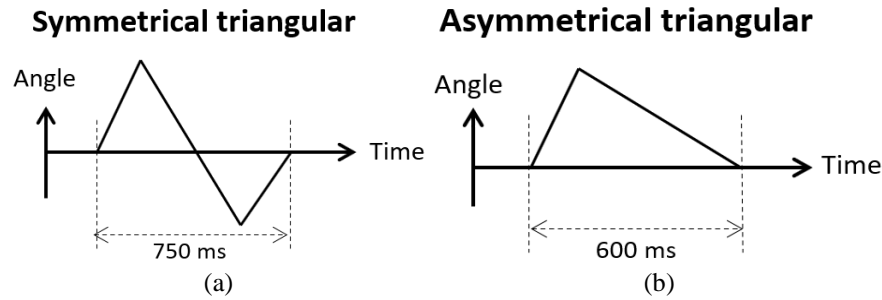


Figure 7. Counter-slippage input signals: (a) symmetrical triangular form and (b) asymmetrical triangular form

2.3. Pre-slippage detection

In real life situation, the above-mentioned counter-slippage method should not be activated throughout the whole transportation process, as it will then jeopardize the EOCC trajectory tracking and precision performance. By right, the counter-slippage should be activated only when it is necessary. Therefore, a pre-slippage detection is also proposed in this paper. This detection method is intended to detect the occurrence of slippage or possible slippage. A scanning window is used, in which the latest 20 samples of positional error in the feedback loop of the control system are computed to obtain an average value. If this simple moving average (SMA) value surpasses a pre-set threshold value, then it can be deduced that a slippage occurred or about to occur, and counter-slippage is needed to be activated at that instant. Figure 8 shows a comparison between trajectory tracking performance with and without pre-slippage detection and counter-slippage.

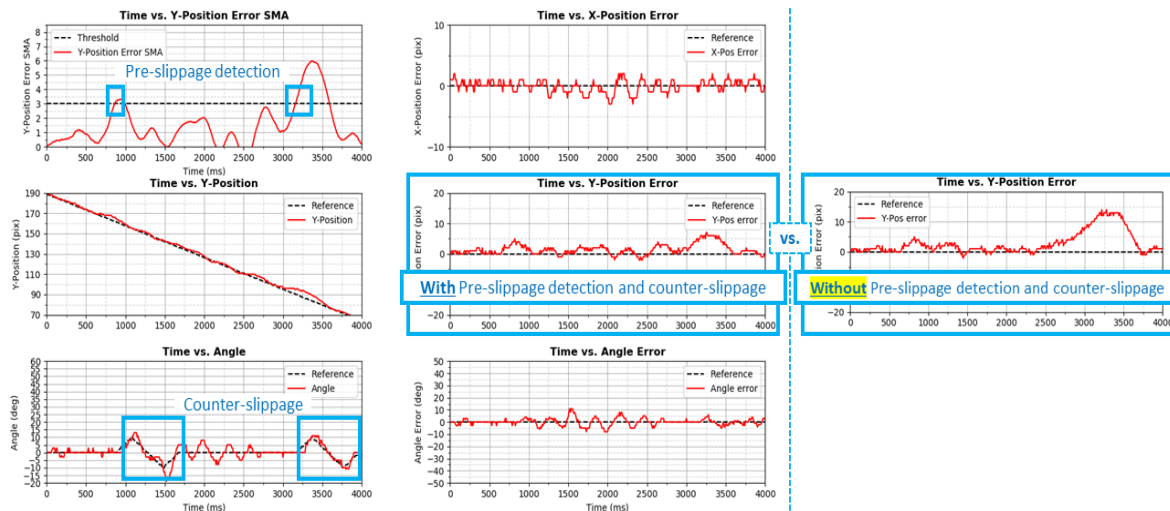


Figure 8. Trajectory tracking performance with and without pre-slippage detection and counter slippage

In Figure 8, it can be noticed that the pre-slippage detector detects the slippage at timestep of around 800 ms and 3200 ms. In the 'Time vs. Angle' plot, symmetrical triangular input of counter slippage was activated at the respectively timesteps. As result, the effect of slippage is mitigated, and the overall tracking performance is improved. Even though the counter-slippage causes some disturbance towards angle control, but it significantly improves the positioning performance. Moreover, the angle control performance remains under-controlled. Therefore, this trade-off is well-worth

3. DESIGN OF EXPERIMENT

To accurately validate the performances of the proposed EOCC, control system, pre-slippage detector, and counter slippage, four trajectories as shown in Figure 9 are used to conduct the experiments. These four trajectories are vertical-left (VL), vertical-right (VR), horizontal-top (HT) and horizontal-bottom

(HB). These four trajectories have shape of alphabet ‘S’ but has different starting position and ending position. Figures 9(a) and (b) illustrate all the S-shaped trajectories i.e. VL, VR, HT and HB used to conduct the experiments. This is because, as mentioned in section 2.1 in this paper, the nominal characteristic of the EOCC is showing system uncertainty and nonlinearity, therefore the performance of the proposed methods should be validated thoroughly across different positions. Each trajectory tracking lasts for 4 seconds in real time. However, in V-REP, the simulation takes about 5 minutes of runtime due to complex computation.

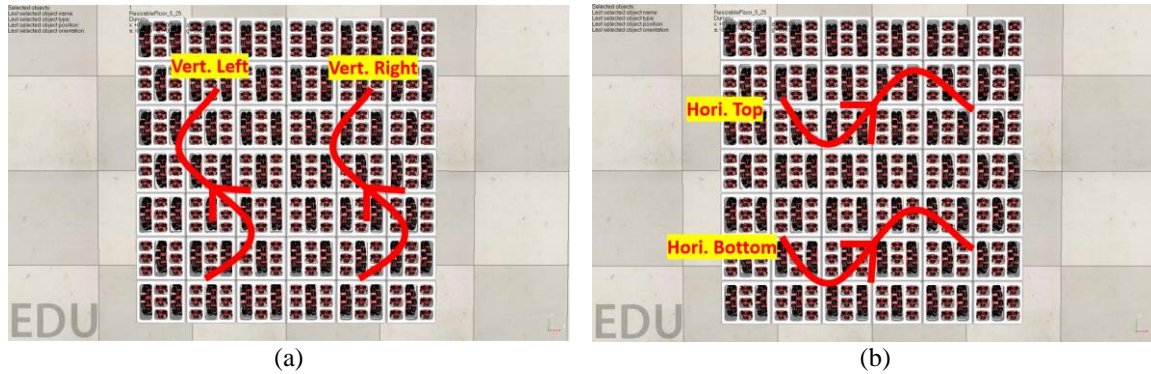


Figure 9. Counter-slippage input signals: (a) symmetrical triangular form and (b) asymmetrical triangular form

To quantify the tracking performance, integral of absolute error (IAE) and integral of squared error (ISE) as shown as (2) and (3) respectively are being used as performance index.

$$IAE = \sum_0^K |e(k)| \quad (2)$$

$$ISE = \sum_0^K (e(k))^2 \quad (3)$$

IAE quantifies the overall performance of the trajectory tracking by simply summing all the absolute error values. Whereas for ISE, all error values are squared before being summed. Therefore, ISE is exponentially more sensitive towards error that is larger than value of 1, which make it suitable to quantify tracking performance that has large error. However, ISE is less sensitive towards error value that is below the value of 1, and that is why both IAE and ISE are needed, working complementarily for each other.

4. RESULTS AND DISCUSSION

Three designs of control system are compared in this section i.e., ‘benchmark’ (BM), ‘symmetrical triangular’ (SY) and ‘asymmetrical triangular’ (ASY), in which the benchmark is the common controller method found in the literature. To achieve fair comparison, these three designs of control system have similar P-P-P-P controller setting, and the box conveyed by the EOCC is at a constant mass of 1kg and constant size of 0.35 m (width)×0.35m (length)×0.2m (height) throughout all the experiments in this paper. The ‘benchmark’ control system does not have any counter-slippage method implemented. The SY design has pre-slippage detector and counter-slippage input in the shape of symmetrical triangle, whereas the ASY design uses asymmetrical triangular signal, as mentioned in section 2 in this paper. Hypothetically, the ‘benchmark’ should have the least satisfactory performance among all due to its non-counteractive design towards wheel slippage. Figures 10 to 13 shows the performances in of the EOCC in trajectories vertical-left (VL), vertical-right (VR), horizontal-top (HT) and horizontal-bottom (HB), respectively. Their IAE and ISE performance index can be found from Tables 1 to 4.

Based on Figure 10, it can be observed that the pre-slippage detector detected slippage twice. The counteractive performance of the counter-slippage methods is highlighted and compared in the yellow box drawn in the plot. Both SY and ASY had successfully reduced the destructive effect caused by the slippages, general improvement of 42% and 73% in term of IAE and ISE, respectively. This statement can be further justified by looking at the ‘Y-position error’ in Table 1. Both SY and ASY have almost similar achievement, but in term of ‘Angle error’, it can be observed that ASY caused higher peak of angle error during the

counter-slippage process. However, based on the IAE, both are very much comparable. Besides that, it is important to also discussed that the first slippage triggered as shown in Figure 10 seems like a false alarm. Even though the false alarm did not cause any harm to the positioning performance, but it significantly affected the angle control performance.

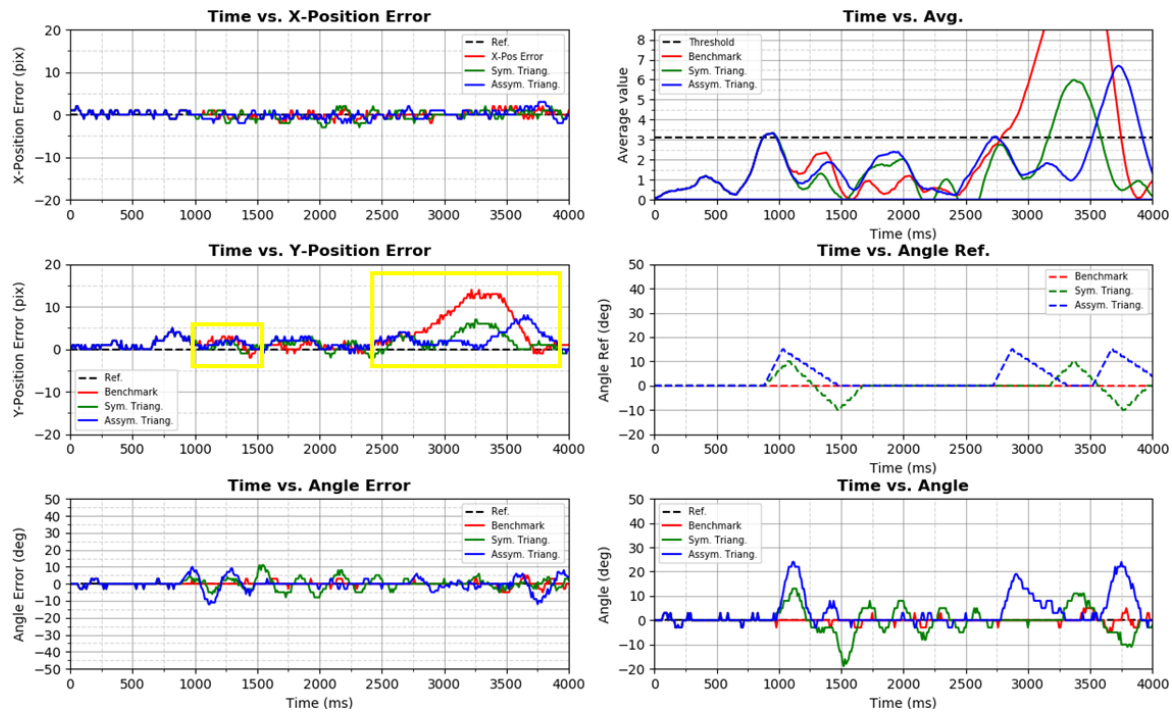


Figure 10. Performance of the EOCC in VL trajectory

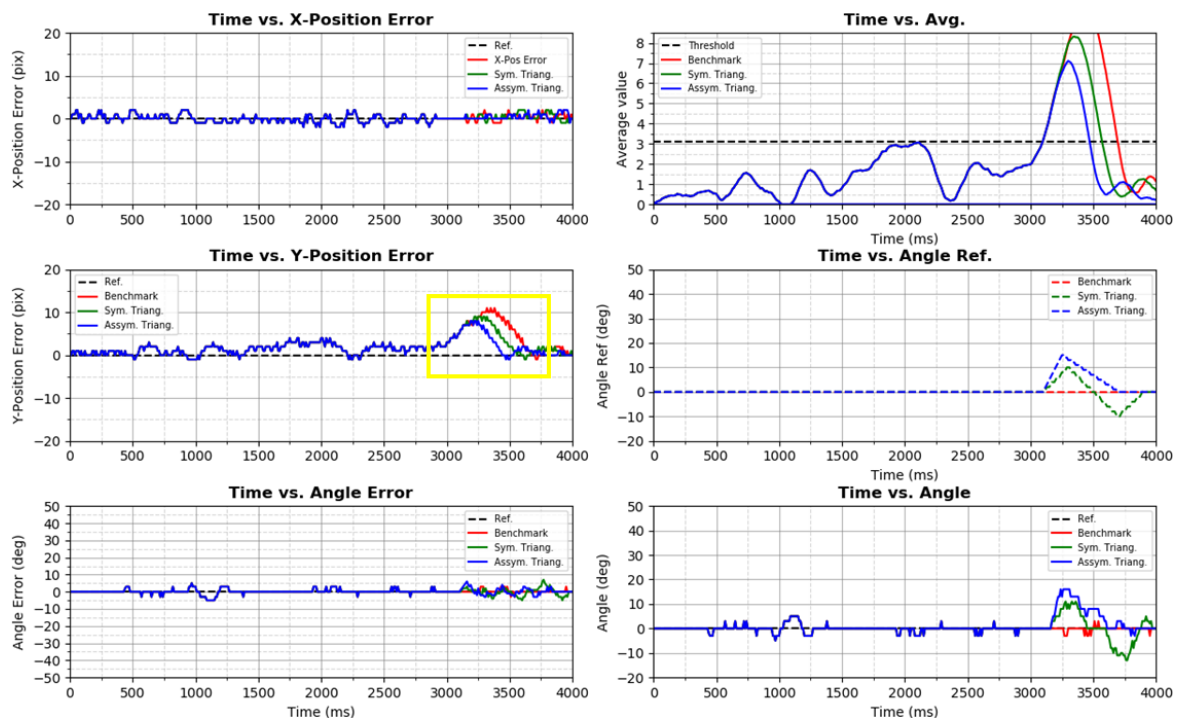


Figure 11. Performance of the EOCC in VR trajectory

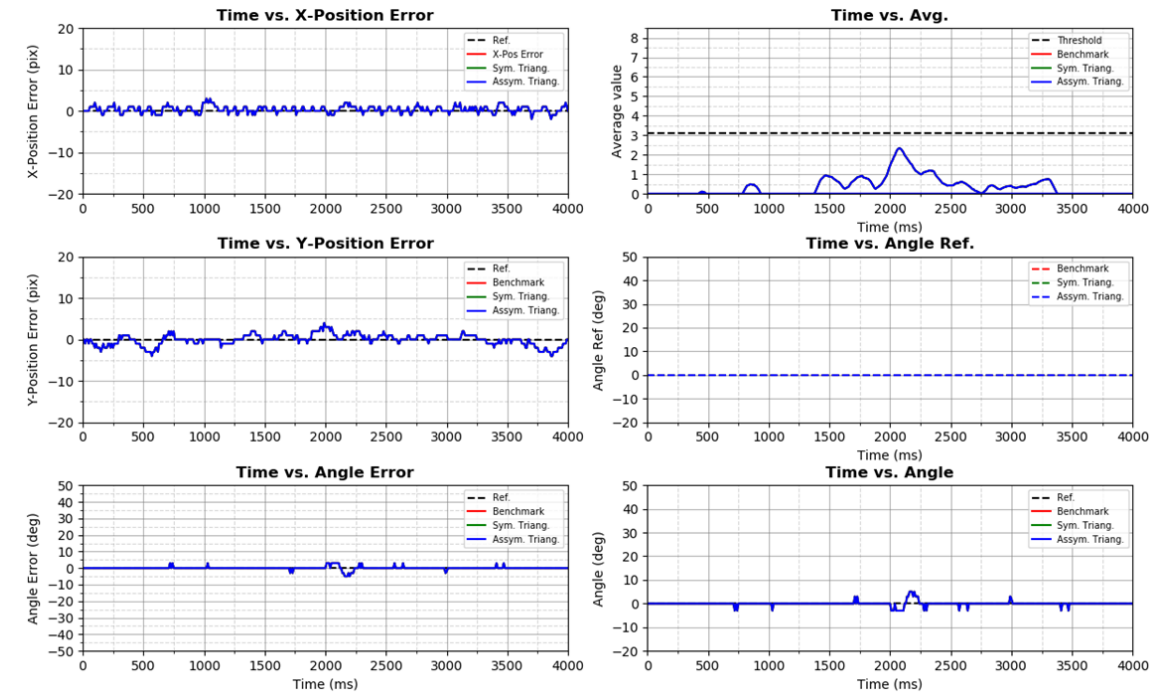


Figure 12. Performance of the EOCC in HT trajectory

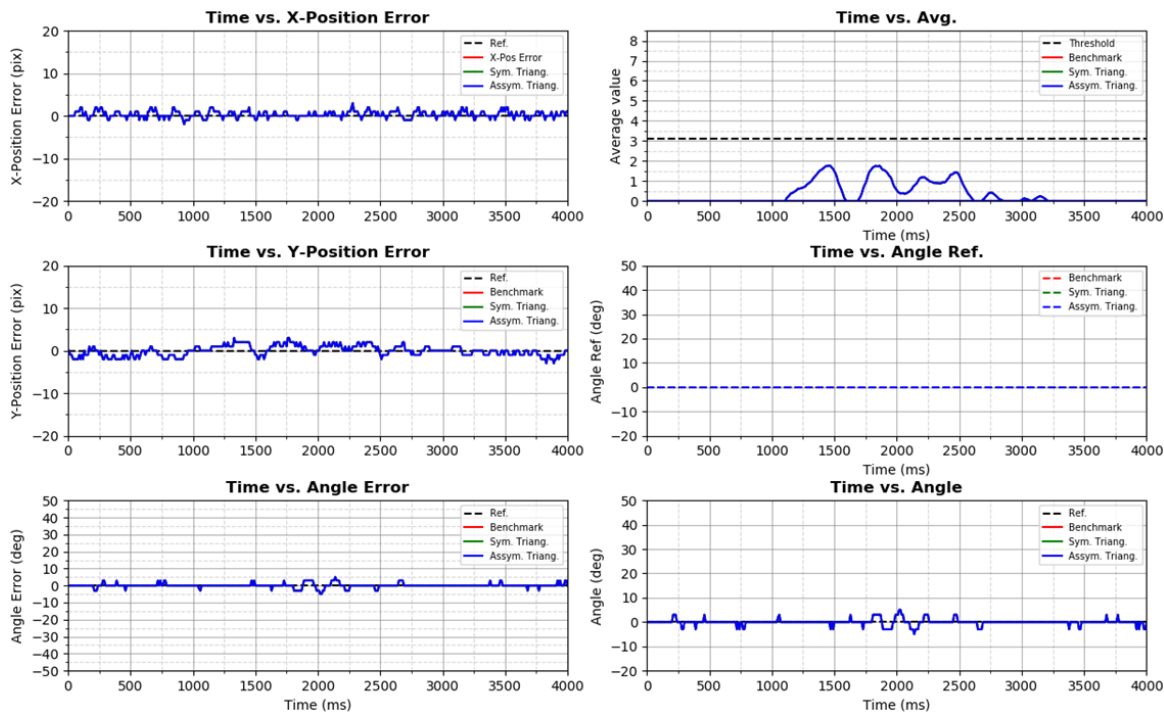


Figure 13. Performance of the EOCC in HB trajectory

Table 1. IAE and ISE for VL trajectory tracking

	Benchmark		Symmetrical triangular		Asymmetrical triangular	
	IAE	ISE	IAE	ISE	IAE	ISE
X-position error	230.0	216.3	299.8	366.3	287.5	348.5
Y-position error	1210.8	9120.2	673.0	2067.7	736.8	2374.2
Angle error	237.0	813.0	1293.0	10219.0	1490.0	20974.0

Table 2. IAE and ISE for VR trajectory tracking

	Benchmark		Symmetrical triangular		Asymmetrical triangular	
	IAE	ISE	IAE	ISE	IAE	ISE
X-position error	273.0	295.2	270.0	297.4	269.1	298.7
Y-position error	914.6	4416.0	790.5	3097.3	700.7	2295.0
Angle error	210.0	708.0	615.0	4311.0	626.0	5506.0

Table 3. IAE and ISE for HT trajectory tracking

	Benchmark		Symmetrical triangular		Asymmetrical triangular	
	IAE	ISE	IAE	ISE	IAE	ISE
X-position error	264.2	280.2	264.2	280.2	264.2	280.2
Y-position error	394.4	686.9	394.4	686.9	394.4	686.9
Angle error	106.0	356.0	106.0	356.0	106.0	356.0

Table 4. IAE and ISE for HB trajectory tracking

	Benchmark		Symmetrical triangular		Asymmetrical triangular	
	IAE	ISE	IAE	ISE	IAE	ISE
X-position error	261.4	273.1	261.4	273.1	261.4	273.1
Y-position error	388.0	561.7	388.0	561.7	388.0	561.7
Angle error	203.0	637.0	203.0	637.0	203.0	637.0

Based on Figure 11, which is the result of VR trajectory tracking, both SY and ASY demonstrated significant counter-slippage effectiveness when compared with BM. It is also significant that the ASY performed better than SY – faster recovery from slippage. Quantitatively, in term of ‘Y-position error’, SY and ASY is 14% and 23% respectively better than BM in IAE, 30% and 48% respectively in ISE.

In HT trajectory tracking result as shown in Figure 12 and Table 3, since there were no happening of slippage, therefore, all three experiments i.e., BM, AS and ASY produced similar tracking performance.

Based on the result shown in Figure 13, there are also no slippage detected in the tracking performance of HB trajectory. Therefore, BM, SY and ASY all have similar tracking result. Overall, based on all the findings in this result section, it can be concluded that the proposed counter-slippage is effective, which can be seen in VL and VR experiments. The ASY counter-slippage method produced the most consistent satisfactory trajectory tracking performance among all. Anyhow, if the angle control performance is a major concern, SY counter-slippage method could be the better alternative.

Based on all the trajectory tracking results presented in this section, it can be observed that both SY and ASY yield a better performance than the BM. Working together with the proposed pre-slippage detector as well, both SY and ASY successfully mitigate the negative impact of slippage with quick recovery. As mentioned in the last section, the process of designing SY and ASY do not require complex mathematical modelling, thus making it quick and suitable for industrial applications. Therefore, through these proposed methods, the contributions presented in this paper aspire to drive the current infancy stage of OCC industry one step closer towards broad adoption and wide implementation.

5. CONCLUSION

In this paper, pre-slippage detector and counter-slippage are introduced into the existing control system of EOCC. The pre-slippage detector utilizes a simple moving average window to scan and determine the possible occurrence of slippage. Whereas for the counter-slippage methods proposed in this paper, two types of counter-slippage method i.e. symmetrical triangular input signal and asymmetrical triangular input signal were proposed and validated. The overall result shows that slippage had been successfully reduced with the help of these proposed methods.

In the future, weighted moving average can be used, which is more sensitive and accurate on incoming slippage data. Then, to match with real-life logistics situation, the properties of the box such as mass and size will be changed. The current control system for EOCC is expected to be optimized as well. Such new control system is expected to be adaptive and robust towards variations. Finally, multiple boxes will be introduced to demonstrate parallel omnidirectional transportation.

ACKNOWLEDGEMENTS

The authors wish to express their gratitude to Motion Control Research Laboratory (MCon Lab), Center for Robotics and Industrial Automation (CeRIA), Centre for Research and Innovation Management

(CRIM), Faculty of Electrical Technology and Engineering (FTKE), and Universiti Teknikal Malaysia Melaka (UTeM) for supporting the research and publication




REFERENCES

- [1] J. G. Ziegler, N. B. Nichols, and N. Y. Rochester, "Optimum settings for automatic controllers," *Journal of Dynamic Systems, Measurement and Control*, vol. 115, pp. 759–768, 1942.
- [2] A. W. Youssef, N. M. Elhusseiny, O. M. Shehata, L. A. Shihata, and E. Azab, "Kinematic modeling and control of omnidirectional wheeled cellular conveyor," *Mechatronics*, vol. 87, 2022, doi: 10.1016/j.mechatronics.2022.102896.
- [3] R. L. Williams, B. E. Carter, P. Gallina, and G. Rosati, "Dynamic model with slip for wheeled omnidirectional robots," *IEEE Transactions on Robotics and Automation*, vol. 18, no. 3, pp. 285–293, 2002, doi: 10.1109/TRA.2002.1019459.
- [4] X. Wang, X. T. R. Kong, G. Q. Huang, and H. Luo, "Cellular Warehousing for Omnichannel Retailing: Internet of Things and Physical Internet Perspectives," *5th International Physical Internet Conference*, pp. 1–16, 2018.
- [5] C. N. Wang, Y. H. Wang, H. P. Hsu, and T. T. Trinh, "Using rotacaster in the heuristic preemptive dispatching method for conveyor-based material handling of 450 mm wafer fabrication," *IEEE Transactions on Semiconductor Manufacturing*, vol. 29, no. 3, pp. 230–238, 2016, doi: 10.1109/TSM.2016.2587755.
- [6] C. Uriarte, A. Asphandiar, H. Thamer, A. Benggolo, and M. Freitag, "Control strategies for small-scaled conveyor modules enabling highly flexible material flow systems," *Procedia CIRP*, vol. 79, pp. 433–438, 2019, doi: 10.1016/j.procir.2019.02.117.
- [7] N. H. Thai, T. T. K. Ly, and L. Q. Dzung, "Trajectory tracking control for mecanum wheel mobile robot by time-varying parameter PID controller," *Bulletin of Electrical Engineering and Informatics*, vol. 11, no. 4, pp. 1902–1910, 2022, doi: 10.11591/eei.v11i4.3712.
- [8] S. Siregar, M. I. Sani, and S. T. P. Silalahi, "Single camera depth control in micro class ROV," *Telkomnika (Telecommunication Computing Electronics and Control)*, vol. 18, no. 3, pp. 1546–1552, 2020, doi: 10.12928/TELKOMNIKA.v18i3.14885.
- [9] H. Oyobe and Y. Hori, "Object conveyance system "Magic Carpet" consisting of 64 linear actuators-object position feedback control with object position estimation," *IEEE/ASME International Conference on Advanced Intelligent Mechatronics. Proceedings*, pp. 1307–1312, doi: 10.1109/AIM.2001.936914..
- [10] Z. Seibold, T. Stoll, and K. Furmans, "Layout-optimized sorting of goods with decentralized controlled conveying modules," *SysCon 2013 - 7th Annual IEEE International Systems Conference, Proceedings*, pp. 628–633, 2013, doi: 10.1109/SysCon.2013.6549948.
- [11] S. Sakunke *et al.*, "Omni-directional conveyor platform: A review paper from automated sorting system and operation research perspective," *International Journal of Innovative Research in Technology*, vol. 5, no. 10, pp. 207–215, 2019.
- [12] L. Overmeyer, K. Ventz, S. Falkenberg, and T. Krühn, "Interfaced multidirectional small-scaled modules for intralogistics operations," *Logistics Research*, vol. 2, no. 3–4, pp. 123–133, 2010, doi: 10.1007/s12159-010-0038-1.
- [13] P. N. F. M. Shamsuddin, R. M. Ramli, and M. A. Bin Mansor, "Navigation and motion control techniques for surface unmanned vehicle and autonomous ground vehicle: A review," *Bulletin of Electrical Engineering and Informatics*, vol. 10, no. 4, pp. 1893–1904, 2021, doi: 10.11591/EEI.V10I4.3086.
- [14] S. H. Mayer, "Development of a completely decentralized control system for modular continuous conveyors," *Universitätsverlag Karlsruhe*, 2009.
- [15] T. Krühn, S. Sohr, and L. Overmeyer, "Mechanical feasibility and decentralized control algorithms of small-scale, multi-directional transport modules," *Logistics Research*, vol. 9, no. 1, 2016, doi: 10.1007/s12159-016-0143-x.
- [16] T. Krühn, S. Falkenberg, and L. Overmeyer, "Decentralized control for small-scaled conveyor modules with cellular automata," *2010 IEEE International Conference on Automation and Logistics, ICAL 2010*, pp. 237–242, 2010, doi: 10.1109/ICAL.2010.5585288.
- [17] J. S. Keek, M. S. M. Aras, Z. Md. Zain, M. B. Bahar, S. L. Loh, and S. H. Chong, "Vision optimization for altitude control and object tracking control of an autonomous underwater vehicle (auv)," *Lecture Notes in Electrical Engineering*, vol. 666, pp. 25–36, 2021, doi: 10.1007/978-981-15-5281-6_3.
- [18] J. S. Keek, S. L. Loh, and S. H. Chong, "Design and control system setup of an E-pattern omniwheeled cellular conveyor," *Machines*, vol. 9, no. 2, pp. 1–33, 2021, doi: 10.3390/machines9020043.
- [19] J. S. Keek, S. L. Loh, and S. H. Chong, "Comprehensive Development and Control of a Path-Trackable Mecanum-Wheeled Robot," *IEEE Access*, vol. 7, pp. 18368–18381, 2019, doi: 10.1109/ACCESS.2019.2897013.
- [20] J. Grabowiecki, "Vehicle wheel," 1919.
- [21] K. Furmans, F. Schonung, and K. R. Gue, "Plug-and-work material handling systems," 2010.
- [22] K. Furmans, C. Nobbe, and M. Schwab, "Future of Material Handling - modular, flexible and efficient," *Proceedings of the IEEE/RSJ International Conference on Intelligent Robots and Systems*, 2011.
- [23] M. B. Firvida, H. Thamer, C. Uriarte, and M. Freitag, "Decentralized omnidirectional route planning and reservation for highly flexible material flow systems with small-scaled conveyor modules," *IEEE International Conference on Emerging Technologies and Factory Automation, ETFA*, vol. 2018, pp. 685–692, 2018, doi: 10.1109/ETFA.2018.8502655.
- [24] L. Ferrière, P. Fisette, B. Raucourt, and B. Vaneghem, "Contribution to the Modelling of a Mobile Robot Equipped with Universal Wheels," *IFAC Proceedings Volumes*, vol. 30, no. 20, pp. 675–682, 1997, doi: 10.1016/s1474-6670(17)44335-7.
- [25] S. L. Dickerson and B. D. Lapin, "Control of an omni-directional robotic vehicle with Mecanum wheels," pp. 323–328, 1991, doi: 10.1109/ntc.1991.148039.
- [26] M. De Villiers and N. S. Tlale, "Development of a control model for a four wheel mecanum vehicle," *Journal of Dynamic Systems, Measurement and Control, Transactions of the ASME*, vol. 134, no. 1, 2012, doi: 10.1115/1.4005273.
- [27] B. E. Ilon, "Wheels for a course stable selfpropelling vehicle movable in any desired direction on the ground or some other base," *Bromma, Sweden*, pp. 1–8, 1975.
- [28] O. Bayasli and H. Salhi, "The cubic root unscented kalman filter to estimate the position and orientation of mobile robot trajectory," *International Journal of Electrical and Computer Engineering*, vol. 10, no. 5, pp. 5243–5250, 2020, doi: 10.11591/IJECE.V10I5.PP5243-5250.
- [29] R. Bangal, S. Nalawade, and C. Dusane, "Design and Control of Omnidirectional Conveyor Model Using Image Processing," *2023 Somaiya International Conference on Technology and Information Management, SICTIM 2023*, pp. 44–49, 2023, doi: 10.1109/SICTIM56495.2023.10104684.




- [30] A. Andreev and O. Peregudova, "On the Trajectory Tracking Control of a Wheeled Mobile Robot Based on a Dynamic Model with Slip," *Proceedings of 2020 15th International Conference on Stability and Oscillations of Nonlinear Control Systems (Pyatnitskiy's Conference), STAB 2020*, 2020, doi: 10.1109/STAB49150.2020.9140714.
- [31] V. Alakshendra and S. S. Chiddarwar, "A robust adaptive control of mecanum wheel mobile robot: Simulation and experimental validation," *IEEE International Conference on Intelligent Robots and Systems*, vol. 2016-November, pp. 5606–5611, 2016, doi: 10.1109/IROS.2016.7759824.

BIOGRAPHIES OF AUTHORS






Joe Siang Keek    received Bachelor of Mechatronics Engineering and Master of Science in Electrical Engineering from Universiti Teknikal Malaysia Melaka (UTeM) in 2017 and 2019, respectively. He is currently a Ph.D. candidate at Faculty of Electrical Technology and Engineering (FTKE), of UTeM, and is also an engineer in a semiconductor company. His research interests include robotics, automation, control engineering, and statistical analysis. He can be contacted at: keek.j.s@gmail.com.






Ser Lee Loh    received Bachelor of Science (Industrial Mathematics), Master of Science in Mathematics and Doctor of Philosophy in Mathematics from Universiti Teknologi Malaysia (UTM) in 2006, 2007, and 2011, respectively. She is currently a senior lecturer at Faculty of Electrical Technology and Engineering (FTKE) of Universiti Teknikal Malaysia Melaka (UTeM). Her research interests include operational research, optimization, and image processing. She can be contacted at: slloh@utem.edu.my.



Ainain Nur Hanafi    holds a Ph.D. in Electrical Engineering from University of Newcastle, Australia, specialising in fault tolerant control. She currently serving as a lecturer at the Department of Engineering of Faculty of Electrical Technology and Engineering (FTKE) at Universiti Teknikal Malaysia Melaka (UTeM). Her research interests include control system, automation, and energy management system. She can be contacted at: ainain@utem.edu.my.



Tau Han Cheong    received Bachelor of Science (Industrial Mathematics) and Master of Science in Mathematics from Universiti Teknologi Malaysia (UTM) in 2005 and 2007, respectively. He is currently a senior lecturer at Faculty of Education of Universiti Teknologi MARA (UiTM Cawangan Selangor). His research interests include numerical computing, mathematics computing, mathematics education, and operational research. He can be contacted at: cheongtauhan@uitm.edu.my.